

1 Biological Evaluation of Molecules of the azaBINOL Class as Antiviral Agents:
2 Specific Inhibition of HIV-1 RNase H Activity by 7-Isopropoxy-8-(naphth-1-yl)quinoline

3

4

5

6 Ross D. Overacker,¹ Somdev Banerjee,¹ George F. Neuhaus,¹ Selena Milicevic Sephton,¹
7 Alexander Herrmann,² James A. Strother,³ Ruth Brack-Werner,² Paul R. Blakemore,¹ and Sandra
8 Loesgen^{1*}

9

10 ¹Department of Chemistry, Oregon State University, Corvallis, OR 97331, USA.

11 ²Institute of Virology, Helmholtz Zentrum München, German Research Center for
12 Environmental Health, Ingolstädter Landstraße 1, D-85764 Neuherberg, Germany

13 ³Department of Integrative Biology, Oregon State University, Corvallis, OR 97331, USA.

14

15 E-mail: sandra.loesgen@oregonstate.edu

16 KEYWORDS: azaBINOL, HIV-1 inhibition, HIV reverse transcriptase, RNase H

17

18 **Abstract**

19 Inspired by bioactive biaryl-containing natural products found in plants and the marine
20 environment, a series of synthetic compounds belonging to the azaBINOL chiral ligand family
21 was evaluated for antiviral activity against HIV-1. Testing of 39 unique azaBINOLs in a single-
22 round infectivity assay resulted in the identification of three promising antiviral compounds,
23 including 7-isopropoxy-8-(naphth-1-yl)quinoline (azaBINOL **B#24**), which exhibited low-
24 micromolar activity. The active compounds and several close structural analogues were further
25 tested against three different HIV-1 envelope pseudotyped viruses as well as in a full-virus
26 replication system (EASY-HIT). Mode-of-action studies using a time-of-addition assay indicated
27 that azaBINOL **B#24** acts after viral entry but before viral assembly and budding. HIV-1 reverse
28 transcriptase (RT) assays that individually test for polymerase and RNase H activity were used to
29 demonstrate that **B#24** inhibits RNase H activity, most likely allosterically. Further binding
30 analysis using bio-layer interferometry (BLI) showed that **B#24** interacts with HIV-1 RT in a
31 highly specific manner. These results indicate that azaBINOL **B#24** is a potentially viable, novel
32 lead for the development of new HIV-1 RNase H inhibitors. Furthermore, this study
33 demonstrates that the survey of libraries of synthetic compounds, designed purely with the goal
34 of facilitating chemical synthesis in mind, may yield unexpected and selective drug leads for the
35 development of new antiviral agents.

36

37 **1. Introduction**

38
39 HIV/AIDS continues to be a major global health epidemic. In 2017, there were 36.9 million
40 people living with HIV worldwide and an additional 1.8 million people became newly infected.¹
41 Despite substantial efforts towards vaccine development, there are currently no FDA-approved
42 vaccines and management of HIV infection requires long-term treatment with potent anti-HIV
43 drugs.² Although drug regimens such as antiretroviral therapy (ART) are able to keep HIV viral
44 load low in infected patients, these treatments are typically limited by adverse side effects,
45 increasing drug resistance, high costs, and global availability shortages.³ Currently, therapeutic
46 antiviral drugs target different phases of the HIV lifecycle including viral attachment, fusion,
47 reverse transcription, integration, and protease activity. Treatments often utilize multiple drugs in
48 combination to combat the rapid emergence of chemoresistant viruses.³ Therefore, novel
49 therapeutics that act on previously untargeted steps of the viral life cycle are urgently needed to
50 circumvent the onset of drug resistance and to improve treatments.⁴

51 HIV reverse transcriptase (RT) has been successfully targeted with first and second-
52 generation non-nucleosides reverse transcriptase inhibitors (NNRTIs) as exemplified by
53 nevirapine, first introduced in 1996, and more recently rilpivirine, in 2011.^{5,6} Out of the 27
54 currently FDA approved HIV drugs on the market, 13 of them target RT polymerase activity,
55 including the NNRTIs.⁷ However, the reverse transcriptase enzyme is a multifunctional protein
56 and no drugs have been developed yet that target the RT ribonuclease H (RNase H) activity,
57 which has recently been validated as a target for small molecule drug intervention.^{8,9} HIV RT is
58 responsible for converting the single-stranded viral RNA genome to a double-stranded DNA for
59 subsequent integration into the genome of the host cell. The heterodimeric RT protein (p66/p51)
60 has separate active sites for polymerase and RNase H activity. The polymerase starts the

61 synthesis of DNA by first copying the viral RNA genome and forming RNA:DNA hybrids while
62 RNase H catalyzes the degradation of RNA in DNA:RNA hybrids to finally form duplex DNA.¹⁰
63 The RNase H active site contains two bivalent Mg²⁺ ions that chelate and cleave the RNA
64 phosphate backbone by directing a nucleophilic water molecule towards the phosphate linkage.¹¹
65 It has been shown that RNase H activity can be abolished through Mg²⁺ chelation in the active
66 site or through allosteric binding near the NNRTI site causing conformational changes.⁹ The
67 addition of novel antiviral drugs that target RNase H activity to current combinatorial regimens
68 would introduce a new synergistic method of HIV-1 inhibition greatly improving efficacy of
69 treatment options.

70 To identify novel leads for drug discovery efforts one may look to sources of compounds that
71 have been either infrequent explored or else untapped in prior studies. Notable in this regard are
72 the numerous ostensibly artificial organic molecules that have been introduced as chiral metal
73 ligands and/or organocatalysts for the purpose of facilitating catalytic enantioselective syntheses.
74 The structural features present in such molecules that are necessary for their intended function
75 (e.g., chiral scaffolds with few rotatable bonds, donor sites from atoms with lone pairs, hydrogen-
76 bond acceptors and donors, sites of localized charge density, zones of steric encumbrance, etc.)
77 could also lead to meaningful and potentially specific interactions with proteins and other classes
78 of biomolecules involved in various diseases. Axially chiral biaryl compounds based on 1,1'-
79 binaphthyl scaffolds are considered a 'privileged' class of reagents for enantioselective synthesis
80 and the principal member of this group, 1,1'-bi-2-naphthol (BINOL, **1**), has become one of the
81 most widely used ligands for stoichiometric and catalytic asymmetric reactions.¹² While BINOL
82 itself has previously been found to be cytotoxic, many other biaryl compounds, either found in
83 nature or of artificial origin, have shown potent and selective bioactivities.^{13,14} For example, the

84 axially chiral dimeric naphthylisoquinolone alkaloids first isolated from *Anicistrocladus*
85 *korupensis* in 1991 and later named the michellamines, exhibit selective anti-HIV activity.¹⁵⁻¹⁹
86 Given these facts taken together with the existence of other antiviral biaryl natural products (e.g.,
87 dioncophylline²⁰) and recently identified synthetic antiviral drug leads with multiple aromatic
88 ring systems (e.g., arbidol,²¹ peptide triazoles,²² rhodanine derivatives,²³ naphthylhydrazones,²⁴
89 and hydroxypyridones²⁵), we elected to test a library of heterocyclic biaryl compounds available
90 to us and belonging to the so-called 'azaBINOL' chiral ligand family for inhibition of HIV-1
91 infection.

92 The azaBINOLs are nitrogenous analogs of BINOL based on isostructural 8-(naphth-1-
93 yl)quinoline (**2**, 8-azaBINOL)²⁶ and 8,8'-biquinolyl (**3**, 8,8'-diazBINOL)²⁷⁻²⁹ motifs (Figure 1).
94 These molecules have been a focus of interest both from a fundamental standpoint^{26, 30, 31} and for
95 their potential utility in enantioselective synthesis,^{32, 33} but prior to this work, studies of any
96 aspect of the biological activity of azaBINOLs had yet to be reported. Herein, we show that
97 deoxy-8-azaBINOL derivatives provide a novel scaffold for the inhibition of HIV-1 RT RNase H
98 activity. Our lead compound, the isopropyl ether derivative of 2'-deoxy-8-azaBINOL (**B#24**),
99 shows unoptimized low micromolar activity (4-9 μ M range) in an HIV single round infectivity
100 assay as well as in fully infectious viral assays with low cytotoxicity and a selectivity index
101 of 14.

102

103 2. Chemistry

104 A significant advantage of the azaBINOL family of molecules as compared to their all
105 carbocyclic BINOL congeners is the ease of derivatization of the quinoline nucleus and therefore
106 the facility with which essentially any position of azaBINOL scaffolds can be decorated with
107 ancillary functionality.²⁹ Of the six compounds of primary interest herein (*vide infra*, see Figure
108 2), only the quinol-type 2'-deoxy-8-azaBINOL carbamate derivative **B#43** was previously
109 described in the literature.²⁶ The five new compounds were prepared from known deoxy
110 azaBINOLs (**4**, **5**, and **6**) via straightforward alkylation and acylation reactions (Scheme 1).
111 Carbamate **B#43**, itself accessed by Suzuki-Miyauri cross-coupling of an 8-iodoquinoline and 1-
112 naphthaleneboronic acid,²⁶ was converted to isopropyl ether **B#24** by saponification to quinol **4**
113 followed by Williamson ether synthesis (Scheme 1). The other four compounds, naphthol-type 2-
114 deoxy-8-azaBINOL derivatives **B#59** and **B#60** and 2-deoxy-8,8'-diazabINOL derivatives **B#57**
115 and **B#58**, were prepared from the corresponding phenols **5** and **6**. As hitherto reported, phenols
116 **5** and **6** are themselves efficiently prepared by N-directed oxidative CH functionalization of 8-
117 (naphth-1-yl)quinoline²⁶ and 8,8'-biquinolyl,²⁹ respectively. All six of the azaBINOLs of main
118 focus were prepared and tested for biological activity in racemic form. The configurational
119 stability of these axially chiral compounds has yet to be determined, however, their racemization
120 half-lives are likely to be significantly higher than those of quinol **4** [$\tau_{1/2(\text{rac.})} = 120$ h in MeOH at
121 24 °C] and naphthol **5** [$\tau_{1/2(\text{rac.})} = 89$ h in MeOH at 24 °C] which have been measured as
122 indicated.²⁶

123 3. Results

124 3.1 HIV-1 *in vitro* activity screening of azaBINOL compounds

125 A library of 39 unique azaBINOLs and two BINOLs was screened for antiviral HIV-1
126 activity using a pseudo-typed viral particle, single round infectivity assay (HIVpp) (see
127 Supporting Information for full screening data and structures of all library members; all
128 compounds were screened in racemic form and four were additionally evaluated as their
129 enantiopure (*aS*)- and (*aR*)-atropisomers). Antiviral activity was compared directly to compound
130 cytotoxicity using a standard MTT-based cell viability assay to assess selectivity indices of
131 compounds. Initial screening efforts at single-dose concentrations (10 µg/mL) of the full
132 compound library revealed three compounds with low micromolar anti-HIV activity: **B#24**,
133 **B#43**, and **B#60** (Figure 2). These compounds, an isopropyl ether (**B#24**) and two carbamate
134 derivatives (**B#43** and **B#60**) of deoxy-8-azaBINOL molecules, showed high viral inhibitory
135 activity with only minor cytotoxicity and warranted further investigation. Closer analysis of the
136 compound library revealed three additional azaBINOLs sharing similar structural features to the
137 aforementioned active compounds: a naphthol-type regioisomer of quinol-type ether **B#24**
138 (**B#59**), as well as 2-deoxy-8,8'-diazabinol congeners of the isopropyl ethers and carbamates
139 (**B#57** and **B#58**). Despite the close structural similarities of these compounds, they showed little
140 antiviral activity as compared to **B#24**, **B#43**, and **B#60** (Figure 2). HIV antiviral activity was
141 evident for the isopropyl ether and carbamate derivatives of 2- and 2'-deoxy-8-azaBINOL but it
142 was notably completely absent for the corresponding 2-deoxy-8,8'-diazabinol series of
143 compounds. Due to the close structural similarities between the active isopropyl ether and
144 carbamate compounds to their non-active counterparts in the HIVpp assay, we decided to move
145 all six compounds forward for further activity explorations.

146 Antiviral activity of the isopropyl ether compounds **B#24**, **B#59**, **B#57** and the carbamate
147 derivatives **B#43**, **B#60**, and **B#58** was assessed against three different HIV-1 enveloped pseudo-

148 typed particles with differing tropism including HXB2, YU2, and 89.6 (Table 1). All six of the
149 azaBINOL compounds showed similar activities across all viral variants. Quinol-type 2'-deoxy-
150 8-azaBINOL ether **B#24** in particular showed low micromolar HIV-1 neutralization against each
151 of the strains tested with activity similar to other antiviral drugs such as abacavir.³⁴ Although the
152 naphthol-type 2-deoxy-8-azaBINOL ether **B#59** did show minor antiviral activity at high
153 concentrations, its IC₅₀ was greater than the concentrations tested and significantly larger in
154 comparison to the closely related quinol-type ether **B#24**, which has an IC₅₀ value of 4 - 8 μM.
155 The significant difference in antiviral activity of these two regioisomers (**B#24** and **B#59**) hints
156 towards a highly specific and selective mode of inhibition. The corresponding carbamate
157 derivatives of deoxy-8-azaBINOLs, **B#43** and **B#60**, both showed moderate antiviral activity
158 against all three viral strains but with smaller selectivity indices. Again, neither of the 2-deoxy-
159 8,8'-diazabINOL derivatives, **B#57** or **B#58**, showed any antiviral activity at concentrations up
160 to 200 μM.

161 Next we used the EASY-HIT full viral infection assay system³⁵ to test all six isopropyl ether
162 and carbamate azaBINOL derivatives against fully-infectious, replication competent HIV-1_{LAI}
163 (Table 2). The quinol-type 2'-deoxy-8-azaBINOL ether **B#24** continued to exhibit low
164 micromolar antiviral activity in the EASY-HIT assay system in accordance with results obtained
165 from the HIVpp assay. Surprisingly, the naphthol-type 2-deoxy-8-azaBINOL ether **B#59**
166 exhibited increased antiviral activity. The deoxy-8-azaBINOL carbamate derivatives **B#43** and
167 **B#60** gave similar high micromolar viral neutralization but also displayed comparable
168 cytotoxicity. The analogous 2-deoxy-8,8'-diazabINOL compounds, **B#57** and **B#58**, showed no
169 antiviral activity or cytotoxicity at concentrations tested up to 200 μM.

170 Out of the 41 unique compounds originally screened for anti-HIV-1 activity, one compound,
171 quinol-type 2'-deoxy-8-azaBINOL ether **B#24**, stands out with selective antiviral activity and a
172 favorable selectivity index. Small changes to its structure, including moving the isopropyl ether
173 substituent to the naphthyl ring system (**B#59**), or the introduction of an additional aromatic ring-
174 bound nitrogen atom (**B#57**), results in drastically reduced antiviral activity. While the deoxy-8-
175 azaBINOL carbamate derivatives **B#43** and **B#60** do exhibit antiviral activity in the phenotypic
176 assays, they also show significant cytotoxicity and therefore their apparent antiviral activity is
177 likely due to interference with the cell-based assay. The low micromolar antiviral activity of lead
178 compound **B#24** encouraged us to explore its mode-of-action.

179 **3.2 AzaBINOLS are not pan-assay interference compounds (PAINS)**

180 Promiscuous inhibitors in high-throughput screening endeavors often lead to unproductive
181 identification and development of compounds with non-specific activity.³⁶ For example, cell-
182 based assays requiring a colorimetric out-read can be inhibited through non-specific mechanisms
183 giving false-positive results.³⁷ The cell-based HIVpp used in this study contains a luciferase
184 reporter out read, so we looked to test the capacity of **B#24** to directly inhibit luciferase
185 luminescence in a recombinant luciferase enzyme test (SI Figure 6).³⁸ **B#24** showed no inhibition
186 of luciferase activity nor quenching at any concentrations tested verifying that it was not acting
187 on luminescence. Additionally, based on the low solubility and largely hydrophobic surface area
188 of **B#24**, we sought to probe its ability to inhibit HIV-1 through unspecific aggregation effects.
189 We tested the ability for **B#24** to aggregate at higher concentrations in aqueous conditions via an
190 ¹H-NMR dilution study (SI Figure 7).³⁹ Five concentrations of **B#24** were tested from 200 μ M to
191 12 μ M in 50 mM phosphate buffer made with D₂O and 1% DMSO-d₆. No changes were seen in

192 the number of resonances, peak shape, or chemical shift values indicating that **B#24** does not
193 aggregate under the test conditions.

194 **3.3 Time-of-addition assay**

195 The single round infectivity assay using HIV-1 enveloped pseudotyped viruses is able to
196 report on inhibition of early stages of infection including cell entry, reverse transcription, and
197 integration steps. The active azaBINOL compound **B#24** inhibited all HIV-1 strains tested
198 regardless of their differing viral tropism (HXB2, YU2, and 89.6). This broad inhibition
199 indicated that the antiviral mode-of-action is unlikely to rely on the viral fusion process, as
200 changing the surface glycoprotein does not affect antiviral activity. Additionally, the EASY-HIT
201 assay indicated that **B#24** is active prior to viral packing and budding. To further delineate the
202 stage of the virus replication cycle inhibited by **B#24**, a time-of-addition assay was performed
203 using HIV-1 pseudotyped particles. Compound **B#24** as well as the standard inhibitors temsavir
204 and efavirenz were added at different time points post exposure of the cell to virus to evaluate
205 their inhibitory activity throughout viral infection (Figure 3). Our results show that **B#24** does
206 not act on the initial viral-entry step when compared to the activity of HIV-1 entry inhibitor
207 temsavir, which loses activity if dosed post viral entry. Instead, **B#24** remains active throughout
208 the assay, but exhibits a subtle decrease in antiviral activity between 6-8 hours post infection.
209 Next, we sought to explore viral enzyme interactions directly to verify if **B#24** interacts with the
210 HIV RT dual functions (DNA polymerase and/or RNase H activity) or HIV integrase.

211 **3.4 Activity of B#24 against HIV-1 reverse transcriptase**

212 NNRTI binding to the HIV RT enzyme occurs at a distant, allosteric binding site and the
213 long-distance effects on the RT polymerase activity are well documented.¹⁰ In contrast, inhibitors
214 of the HIV RT enzyme that target its RNase H function directly affect the catalytic side with its

215 Mg^{2+} ions, and therefore are often dual inhibitors, with effects on reverse transcriptase and
216 integrase as both require bivalent metals in their active site. We screened **B#24** for inhibitory
217 activity in recombinant protein-based assays to test for HIV-1 RT and/or integrase antiviral
218 inhibition (Table 3). AzaBINOL **B#24** showed no effect against HIV-1 integrase activity in a
219 commercially available kit (ExpressBio, Frederick, MD) at any concentration tested up to 200
220 μM . When tested against an HIV-1 RT polymerase assay we observed only weak inhibitory
221 effects for **B#24** at concentrations higher than 100 μM , several orders of magnitude weaker than
222 seen in our cell-based assays.

223 However, since RNase H activity, the second catalytic activity of the HIV-1 reverse
224 transcriptase, is not detected in the above RT-polymerase assay, we investigated the effect of
225 **B#24** on RNase H activity using a previously reported FRET based approach.^{40, 41} Here, we used
226 a pair of oligonucleosides including an 18-mer strand of RNA containing a 3'-fluorescein
227 modification and an 18-mer strand of DNA with a 5'-dabcyl quencher modification. When RNA
228 is cleaved from the RNA/DNA hybrid by RNase H activity, the fluorescent probe is removed
229 from its quenching partner (dabcyl) resulting in fluorescence. We found that **B#24** inhibited
230 RNase H activity of HIV RT with an IC_{50} of 14.2 μM , within the same range as the low
231 micromolar cell-based assay results (Table 3).

232 Several classes of compounds have shown promising antiviral activity by acting on RNase H
233 activity including N-hydroxyimides,⁴² tropolones,^{43, 44} hydroxypyridonecarboxylic acids,^{25, 45, 46}
234 diketoacids,⁴⁷ vinylogous ureas,⁴⁸ and thienopyrimidinones;⁴⁹ the majority of which target the
235 active site of RNase H through Mg^{2+} ion chelation. With this in mind, we sought to probe
236 whether azaBINOL **B#24** was inhibiting RNase H via the active site using a Mg^{2+} ion chelation
237 and absorbance test. Mg^{2+} ions present in the active site of RNase H are an integral part of its

238 endonuclease function and various inhibitors have been shown to interfere with their chelating
239 properties.^{8,9} Compound **B#24** was tested for Mg²⁺ binding by assessment of its UV absorption
240 under an increasing concentration of Mg²⁺ following existing procedures.⁵⁰ No UV absorbance
241 changes were observed with the addition of Mg²⁺ up to 120 mM with **B#24** (100 μM) (Figure 4).
242 Therefore, we conclude that **B#24** is not interacting with Mg²⁺ ions and subsequently is not
243 directly inhibiting RNase H activity through active site binding. Instead, it is likely that **B#24**
244 inhibits RNase H enzyme activity allosterically, without affecting the polymerase function of
245 RT. The azaBINOL compound **B#24** adds a new structural class to emerging group of selective
246 HIV RNase H inhibitors including dihydroxy benzoyl naphthyl hydrazone (DHBNH),²⁴ various
247 derivatives of vinylogous ureas,^{48,51} as well as cycloheptathiophene-3-carboxamides (cHTC).⁵²
248 ⁵³ Allosteric binding may exhibit fewer side effects compared to active site Mg²⁺ chelating
249 inhibitors and therefore allow for a more favorable therapeutic window.^{8,9}

250 **3.5 HIV-1 reverse transcriptase binding**

251 To show that **B#24** inhibits RNase H activity by binding the HIV-1 reverse transcriptase
252 enzyme, we explored direct binding to immobilized HIV-1 RT using bio-layer interferometry
253 (BLI). BLI allows for the real time measurement of binding affinities between ligands and
254 analytes of varying size using single-use, fiber optical sensors. BLI measures association (k_{on})
255 and dissociation (k_{off}) rates directly from full spectrum wavelength shifts associated with
256 interference pattern changes derived from binding events at a sensors tip to determine binding
257 affinities (K_D).⁵⁴ Recombinant-wild type HIV-1 p66/p51 RT (NIH Aids Reagents) was
258 immobilized via amine coupling onto BLI biosensors. **B#24**, selected other azaBINOLs, and
259 control compounds (rilpivirine positive control, raltegravir negative control) were prepared in 1x
260 kinetics buffer at multiple concentrations. Each compound was tested at multiple concentrations,

261 responses were globally fit using a 1:1 binding model, and these fits were used to calculate K_D
262 values. The binding curves obtained for **B#24** are shown in Figure 5. In good agreement with
263 cell-based antiviral assays, **B#24** shows a concentration-dependent binding to HIV-1 RT. Control
264 compound rilpivirine also showed concentration dependent binding curves while raltegravir, an
265 HIV-1 integrase inhibitor showed no binding at any concentration tested as expected (SI Figure
266 4). Although the acquired K_D of 38 μ M associated with **B#24** is higher than the IC_{50} in cell-based
267 assays, it should be noted that the affinity value cannot be directly related to neutralization
268 efficacy, as seen in many high-affinity, non-neutralizing HIV antibodies.⁵⁵⁻⁵⁷ No binding was
269 observed for the related azaBINOLs of interest from the compound library (SI Figure 7). In
270 summary, the BLI binding data obtained reveals a striking correlation between the binding
271 affinity of **B#24** towards its target HIV RT and its antiviral activity.

272 4. Discussion and conclusion

273 RNase H inhibition of HIV-1 RT is an under explored and under-utilized mechanism of
274 inhibition. The azaBINOL compounds reported here represent novel scaffolds that inhibit HIV
275 via an underexplored allosteric mechanism with low toxicity and high specificity. In particular,
276 the isopropyl ether derivative of 2'-deoxy-8-azaBINOL (**B#24**) exhibits with potent and specific
277 antiviral activity against HIV RNase H. We utilized time-of-addition experiments and
278 recombinant enzyme assays to show that **B#24** specifically inhibits RNase H. In addition, we
279 used BLI to show that **B#24** binds to HIV RT via a 1:1 binding mechanism with a binding
280 affinity (K_D) of 38 μ M. Although a number of azaBINOL compounds within the screened library
281 were found to have limited solubility in the cell-based assays as expected, aggregation and non-
282 specific inhibition was tested thoroughly and can be dismissed for lead compound **B#24** (SI Fig
283 6,7).

284 Clinically approved HIV-1 NNRTI's including nevirapine, efavirenz, and recently rilpivirine,
285 exhibit antiviral activity against HIV-1 by allosterically inhibiting RT through hydrophobic
286 interactions at the NNRTI binding site.^{24, 25, 58, 59} Binding to the NNRTI binding site often results
287 in combined effects in inhibiting DNA polymerase and RNase H activity through conformational
288 shifts in the enzyme.⁶⁰ Only a few privileged structures like the acyl hydrazones,²⁴ vinyllogous
289 ureas,⁴⁸ cHTC's,⁵³ and now **B#24** have been identified with potent HIV-1 inhibitory effects
290 through specific RNase H inhibition.

291 We predict that the naphthyl moiety of the azaBINOL compounds may bind to a hydrophobic
292 surface present on the RNase H domain of HIV-1 RT²⁵ while leaving the substituted quinoline
293 space to further interact with the protein. In the case of the 2-deoxy-8,8'-diazabINOL derivatives
294 (**B#57**, **B#58**) or the naphthol-type regioisomer of ether **B#24** (**B#59**), the antiviral activity is
295 absent or significantly reduced likely due to the reduced hydrophobic surface and increased
296 steric interactions, respectively. Ongoing research in our laboratory will explore if **B#24** truly
297 binds allosterically to RNase H and if the binding affinity and HIV-1 neutralization can be
298 enhanced by chemical modifications.

299 Future studies are planned to optimize the azaBINOL core structure to increase HIV-1
300 activity by improving HIV-1 binding, solubility, and to reduce cytotoxicity. It is anticipated that
301 the absolute configuration of the biaryl system will influence biological activity but to what
302 extent remains an open question since a majority of the compounds evaluated herein were tested
303 in racemic form only. Work is in progress to determine the configurational stability of
304 compounds such as **B#24** and bioassays of these materials in enantioenriched form will be
305 conducted should their racemization half-lives prove to be high enough for such an effort to be
306 meaningful.

307 In summary, we discovered that an isopropyl ether derivative of an aza-analog of the
308 archetypal axially chiral biaryl ligand BINOL, inhibits HIV-1 infection in vitro. Based on the
309 identified RNase H inhibition, direct HIV-1 RT binding, and the known hydrophobic binding
310 surfaces associated with allosteric inhibition,⁵⁸ we believe that **B#24** is a novel allosteric inhibitor
311 of HIV-1 RT-RNase H activity. While biaryl compounds of natural origin have long been known
312 to exhibit significant biological activity,^{14, 61} this study suggests that further investigations of the
313 bioactivity of artificial biaryls, designed purely with synthetic utility in mind, are warranted.

314 **5. Experimental Section**

315 **5.1 General experimental procedures.**

316 UV spectra, luminescence and absorbance readings were recorded on a BioTek Synergy HT
317 plate reader. NMR spectra were acquired on Bruker Avance III 400 MHz, Bruker Avance III 500
318 MHz, Bruker Avance III 700 MHz, and Bruker Ascend 800 MHz spectrometers, equipped with
319 either a 5 mm TXI probe (500 MHz), a 5 mm BBO probe (400 MHz and 500 MHz), or a 5 mm
320 TCI cryoprobe (700 MHz and 800 MHz), with the appropriate solvent signals used as an internal
321 calibration standard [for CDCl₃: δ_{H} (CHCl₃) = 7.26 ppm, δ_{C} (CDCl₃) = 77.2 ppm]. Numbers in
322 parentheses following carbon atom chemical shifts refer to the number of attached hydrogen
323 atoms as revealed by the DEPT spectral editing technique. Infra-red spectra were recorded on a
324 Perkin Elmer Spectrum II FT-IR using a thin film between NaCl plates. Low (MS) and high
325 resolution (HRMS) mass spectra were obtained using electrospray (ES) ionization on a Waters
326 SYNAPT instrument interfaced with a Shimadzu LC20ad liquid chromatograph. Ion
327 mass/charge (*m/z*) ratios are reported as values in atomic mass units. Preparative
328 chromatographic separations were performed on silica gel 60 (35-75 μm) and reactions were

329 followed by TLC analysis using silica gel 60 plates (2-25 μm) with fluorescent indicator (254
330 nm) and visualized by UV or phosphomolybdic acid (PMA).

331 **5.2 Materials.**

332 Non-commercially available BINOL and azaBINOL compounds tested were previously
333 synthesized and characterized at Oregon State University. Preparation details and
334 characterization data for previously undescribed compounds (**B#24**, **B#57**, **B#58**, **B#59**, and
335 **B#60**) are given below. Unless otherwise stated, all solvents were purchased from ThermoFisher
336 Scientific (Waltham, MA) and reagents for chemical synthesis were purchased from Sigma-
337 Aldrich (Milwaukee, WI) and used as received. TZM-bl cells and the HIV-1 inhibitors
338 raltegravir, efavirenz, and rilpivirine were obtained through the NIH Aids Reagent Program.⁶²⁻⁶⁷
339 HEK 293T cells were a kind gift from Dr. Pастey Manoj (Oregon State University). HIV-1 viral
340 expression plasmids (pSG3, pHxB2, and pYU2) were obtained as a generous gift from Carole
341 Bewley (NIH, NIDDK). Dulbecco's modified eagle medium (DMEM) was purchased from VWR.
342 PBS buffer was purchased from Gibco (ThermoFisher Scientific). Trypsin/EDTA (0.25%/2.21
343 mM) and penicillin/streptomycin solutions were attained from Corning Life Sciences (Corning,
344 NY). Fetal Bovine Serum (FBS) was obtained from Atlanta Biologicals (Flowery Branch, GA).
345 QuantiLum Recombinant Luciferase and the BrightGlo Luciferase Assay System were acquired
346 from Promega (Madison, WI). The HIV-1 inhibitor temsavir was acquired from ViiV Healthcare
347 (Brentford, UK). All compounds received were tested for purity and identity via LCMS analysis
348 before use.

349 **5.3 Synthesis of new compounds and characterization data.**

350 *Representative procedure for preparation of isopropyl ethers. 7-(Isopropoxy)-8-(naphth-*
351 **1-yl)quinoline (B#24)**: A stirred solution of 7-hydroxy-8-(naphth-1-yl)quinoline (**4**, 20 mg,

352 0.074 mmol)²⁶ in reagent grade DMF (0.5 mL) at rt under Ar was treated with NaH (12 mg, 60
353 wt.% in mineral oil, 0.30 mmol). Effervescence was observed. After stirring for 30 min, neat 2-
354 bromopropane (0.030 mL, d = 1.31, 39 mg, 0.317 mmol) was added. The reaction mixture was
355 then heated to 45 °C and stirring continued for 18 h. After this time, the mixture was allowed to
356 cool to rt and partitioned between EtOAc (5 mL) and H₂O (5 mL). The aqueous phase was
357 extracted with EtOAc (5 mL) and the combined organic phases were washed with H₂O (5 mL)
358 and brine (5 mL), then dried (Na₂SO₄) and concentrated *in vacuo*. The residue was purified by
359 column chromatography (SiO₂, eluting with 15-30% EtOAc in hexanes) to afford ether **B#24** (20
360 mg, 0.064 mmol, 86%) as a colorless oil: IR (neat) 2976, 2927, 1610, 1498, 1307, 1259, 1111,
361 773 cm⁻¹; ¹H NMR (400 MHz, CDCl₃) δ 8.76 (1H, dd, *J* = 4.2, 1.8 Hz), 8.17 (1H, dd, *J* = 8.2,
362 1.8 Hz), 7.92 (1H, dm, *J* = 8.3 Hz), 7.90 (2H, d, *J* = 9.0 Hz), 7.61 (1H, dd, *J* = 8.2, 7.0 Hz), 7.47
363 (1H, d, *J* = 9.0 Hz), 7.45 (1H, dd, *J* = 7.0, 1.2 Hz), 7.42 (1H, ddd, *J* = 8.1, 6.7, 1.4 Hz), 7.31-7.21
364 (3H, m), 4.42 (1H, septet, *J* = 6.1 Hz), 1.05 (3H, d, *J* = 6.1 Hz), 0.98 (3H, d, *J* = 6.1 Hz) ppm;
365 ¹³C NMR (175 MHz, CDCl₃) δ 157.6 (0), 150.2 (1), 147.0 (0), 137.9 (0), 133.9 (0), 132.9 (0),
366 129.1 (1), 128.9 (1), 128.5 (1), 128.3 (1), 126.2 (1), 125.8 (1), 125.6 (1), 125.5 (1), 124.1 (0),
367 119.0 (1), 118.5 (1), 72.6 (1), 22.3 (3), 22.2 (3) ppm (aromatic C-atom signals not fully resolved,
368 20 peaks observed for 22 unique C-atoms); MS (ES⁺) *m/z* 314 (M+H)⁺; HRMS (ES⁺) *m/z*
369 314.1544 (calcd. for C₂₂H₂₀NO: 314.1545).

370 **7-(Isopropoxy)-8,8'-biquinolyl (B#57)**: 7-Hydroxy-8,8'-biquinolyl (**6**, 52 mg, 0.191
371 mmol)²⁹ was converted into isopropyl ether **B#57** (46 mg, 0.146 mmol, 77%) by analogy to the
372 synthesis of **B#24** given above. Data for **B#57**: colorless oil; IR (neat) 2925, 1658, 1596, 1496,
373 1272, 1112, 1045, 829, 796 cm⁻¹; ¹H NMR (400 MHz, CDCl₃) δ 8.78 (1H, dd, *J* = 3.9, 1.8 Hz),
374 8.72 (1H, dd, *J* = 4.2, 1.8 Hz), 8.21 (1H, dd, *J* = 8.3, 1.8 Hz), 8.14 (1H, dd, *J* = 8.2, 1.8 Hz), 7.90

375 (1H, dd, 7.2, 2.5 Hz), 7.88 (1H, d, $J = 9.1$ Hz), 7.71-7.65 (2H, m), 7.47 (1H, d, $J = 9.0$ Hz), 7.34
376 (1H, dd, $J = 8.3, 4.2$ Hz), 7.22 (1H, dd, $J = 8.2, 4.2$ Hz), 4.46 (1H, septet, $J = 6.1$ Hz), 1.06 (3H,
377 d, $J = 6.1$ Hz), 0.96 (3H, d, $J = 6.1$ Hz) ppm; ^{13}C NMR (100 MHz, CDCl_3) δ 156.6 (0), 150.7 (1),
378 149.9 (1), 148.8 (0), 147.8 (0), 136.4 (0), 136.3 (1), 136.0 (1), 132.2 (1), 128.8 (1), 128.6 (0),
379 127.7 (1), 127.3 (0), 126.3 (1), 124.2 (0), 120.7 (1), 119.0 (1), 118.2 (1), 72.5 (1), 22.5 (3), 22.3
380 (3) ppm; MS (ES+) m/z 315 (M+H) $^+$; HRMS (ES+) m/z 315.1502 (calcd. for $\text{C}_{21}\text{H}_{19}\text{N}_2\text{O}$:
381 315.1497).

382 **2-(Isopropoxy)-1-(quinol-8-yl)naphthalene (B#59)**: 2-Hydroxy-1-(quinol-8-
383 yl)naphthalene (**5**, 75 mg, 0.276 mmol)²⁶ was converted into isopropyl ether **B#59** (66 mg, 0.211
384 mmol, 76%) by analogy to the synthesis of **B#24** given above. Data for **B#59**: colorless oil; IR
385 (neat) 2976, 2927, 1716, 1593, 1496, 1371, 1235, 798, 750 cm^{-1} ; ^1H NMR (400 MHz, CDCl_3) δ
386 8.80 (1H, dd, $J = 4.2, 1.8$ Hz), 8.24 (1H, dd, $J = 8.3, 1.8$ Hz), 7.94-7.88 (2H, m), 7.84 (1H, dm, J
387 = 8.1 Hz), 7.68-7.64 (2H, m), 7.41 (1H, d, $J = 9.0$ Hz), 7.37 (1H, dd, $J = 8.3, 4.2$ Hz), 7.31 (1H,
388 ddd, $J = 8.0, 6.6, 1.4$ Hz), 7.21 (1H, ddd, $J = 8.5, 6.6, 1.3$ Hz), 7.15 (1H, dm, $J = 8.5$ Hz), 4.36
389 (1H, septet, $J = 6.1$ Hz), 1.05 (3H, d, $J = 6.1$ Hz), 0.89 (3H, d, $J = 6.1$ Hz) ppm; ^{13}C NMR (175
390 MHz, CDCl_3) δ 153.5 (0), 150.3 (1), 147.8 (0), 136.9 (0), 136.3 (1), 134.4 (0), 132.5 (1), 129.6
391 (0), 129.4 (1), 128.6 (0), 128.1 (1), 127.7 (1), 126.3 (1), 126.1 (1), 126.0 (0), 125.9 (1), 123.7 (1),
392 121.0 (1), 118.5 (1), 72.9 (1), 22.6 (3), 22.4 (3) ppm; MS (ES+) m/z 314 (M+H) $^+$; HRMS (ES+)
393 m/z 314.1546 (calcd. for $\text{C}_{22}\text{H}_{20}\text{NO}$: 314.1545).

394 *Representative procedure for preparation of carbamates. 7-[(Diethylamino)carbonyloxy]-*
395 **8,8'-biquinolyl (B#58)**: A stirred solution of 7-hydroxy-8,8'-biquinolyl (**6**, 43 mg, 0.158
396 mmol)²⁹ in pyridine (1.0 mL) at rt under Ar was treated with neat diethylcarbonyl chloride
397 (0.080 mL, $d = 1.07$, 86 mg, 0.632 mmol). The resulting solution was heated to 100 °C and

398 stirred for 24 h. After this time, the mixture was allowed to cool to rt and partitioned between
399 EtOAc (10 mL), H₂O (15 mL) and sat. aq. NaHCO₃ (5 mL). The aqueous phase was extracted
400 with EtOAc (10 mL) and the combined organic phases washed with H₂O (5 mL) and brine (5
401 mL), then dried (Na₂SO₄) and concentrated *in vacuo*. The residue was purified by column
402 chromatography (SiO₂, eluting with 3% MeOH in CH₂Cl₂) to afford carbamate **B#58** (45 mg,
403 0.121 mmol, 77%) as a colorless oil: IR (neat) 2930, 1715, 1594, 1417, 1263, 1208, 1157, 796
404 cm⁻¹; ¹H NMR (400 MHz, CDCl₃) δ 8.81 (1H, dd, *J* = 4.3, 1.7 Hz), 8.79 (1H, dd, *J* = 4.2, 1.7
405 Hz), 8.22 (1H, dd, *J* = 6.6, 1.7 Hz), 8.20 (1H, dd, *J* = 6.5, 1.7 Hz), 7.94 (1H, d, *J* = 8.9 Hz), 7.90
406 (1H, dd, *J* = 8.1, 1.3 Hz), 7.76 (1H, dd, *J* = 7.1, 1.4 Hz), 7.68 (1H, dm, *J* = 7.3 Hz), 7.64 (1H, d, *J*
407 = 8.8 Hz), 7.35 (1H, t, *J* = 4.4 Hz), 7.33 (1H, d, *J* = 4.4 Hz), 3.17-3.06 (2H, m), 2.68 (1H, dq, *J* =
408 14.2, 7.1 Hz), 2.49 (1H, dq, *J* = 14.2, 7.0 Hz), 0.95 (3H, t, *J* = 7.0 Hz), 0.32 (3H, t, *J* = 7.0 Hz)
409 ppm; ¹³C NMR (100 MHz, CDCl₃) δ 153.8 (0), 150.7 (1), 150.3 (1), 150.1 (0), 148.4 (0), 147.5
410 (0), 136.2 (1), 136.2 (1), 135.0 (0), 132.4 (1), 130.4 (0), 128.6 (0), 128.4 (1), 128.1 (1), 126.6 (0),
411 126.3 (1), 123.4 (1), 120.9 (1), 120.4 (1), 41.9 (2), 41.2 (2), 13.3 (3), 13.2 (3) ppm; MS (ES+)
412 *m/z* 372 (M+H)⁺; HRMS (ES+) *m/z* 372.1716 (calcd. for C₂₃H₂₁N₃O₂: 372.1712).

413 **2-[(Diethylamino)oxycarbonyl]-1-(quinol-8-yl)naphthalene (B#60)**: 2-Hydroxy-1-(quinol-
414 8-yl)naphthalene (**5**, 50 mg, 0.184 mmol)²⁶ was converted into carbamate **B#60** (59 mg, 0.159
415 mmol, 86%) by analogy to the synthesis of **B#58** given above. Data for **B#60**: colorless oil; IR
416 (neat) 2973, 2931, 1713, 1419, 1269, 1213, 1159, 982, 799, 750 cm⁻¹; ¹H NMR (400 MHz,
417 CDCl₃) δ 8.83 (1H, dd, *J* = 4.2, 1.8 Hz), 8.23 (1H, dd, *J* = 8.3, 1.8 Hz), 7.96 (1H, d, *J* = 8.9 Hz),
418 7.92 (1H, dd, *J* = 8.1, 1.5 Hz), 7.91 (1H, dm, *J* = 8.2 Hz), 7.74 (1H, dd, *J* = 7.1, 1.5 Hz), 7.65
419 (1H, dd, *J* = 8.1, 7.2 Hz), 7.52 (1H, d, *J* = 8.9 Hz), 7.42 (1H, ddd, *J* = 8.1, 6.3, 1.6 Hz), 7.39 (1H,
420 dd, *J* = 8.2, 4.2 Hz), 7.33-7.24 (2H, m), 3.15-3.08 (2H, m), 2.74 (1H, dq, *J* = 13.9, 6.9 Hz), 2.53

421 (1H, dq, $J = 14.2, 7.3$ Hz), 0.94 (3H, t, $J = 7.0$ Hz), 0.32 (3H, t, $J = 6.9$ Hz) ppm; ^{13}C NMR (100
422 MHz, CDCl_3) δ 154.2 (0), 150.4 (1), 147.2 (2C, 0), 136.7 (1), 135.4 (0), 134.0 (0), 132.6 (1),
423 131.8 (0), 129.2 (1), 128.6 (2C, 0), 128.3 (1), 128.1 (1), 126.5 (1), 126.3 (1), 126.2 (1), 125.1 (1),
424 122.5 (1), 121.2 (1), 42.0 (2), 41.3 (2), 13.3 (2C, 3) ppm; MS (ES+) m/z 371 (M+H) $^+$; HRMS
425 (ES+) m/z 371.1761 (calcd. for $\text{C}_{24}\text{H}_{23}\text{N}_2\text{O}_2$: 371.1760).

426 **5.4 Cell culture.**

427 TZM-bl and HEK 293T cells were grown in DMEM supplemented with 10% (v/v) FBS,
428 penicillin (100 units/mL), and streptomycin (100 $\mu\text{g}/\text{mL}$). Cells were maintained in a humidified
429 incubator at 37°C with 5% CO_2 . The passage number of cells used in experiments never
430 exceeded 20 passages. All cell lines were tested mycoplasma-negative by real-time PCR
431 (MycoSolutions mycoplasma detection kit, Akron Biotech, Boca Raton, FL).

432 **5.5 Pseudovirus production.**

433 HIV-1 pseudotyped viruses were prepared as previously described.⁶⁸ Briefly, HEK 293T
434 cells were transfected with an envelope expression plasmid (pHxB2, pYU2, or p89.6) and an
435 envelope deficient HIV-1 backbone vector (pSG3 $_{\Delta\text{env}}$) using XtremeGENE HP DNA
436 Transfection Reagent (Roche). After 24 hours of incubation at 37°C and 5% CO_2 , the growth
437 media was replaced with fresh media followed by an additional 24 hours of incubation. Cellular
438 supernatant was collected and passed through a 0.45 μm filter to give pseudoviral stock. 1 mL
439 pseudoviral aliquots were stored at -80°C until further use in neutralization assays. Viral strength
440 was determined through TCID₅₀ calculations. TZM-bl cells were plated at 9000 cells per well in
441 white 96 well plates (Greiner Bio-One) and incubated at 37 C, 5% CO_2 for 24 hours. HIV-1
442 pseudoviruses were added over a two-fold dilution series to wells. At 48 hours-post infection,
443 cells were lysed and BrighGlo luciferase substrate (Promega) added. Luminescence reading were

444 immediately recorded and the TCID₅₀ value calculated as 50% of the maximum light output
445 based on control wells.

446 **5.6 HIV-1 pseudovirus single-round infectivity assay.**

447 Viral infection rates of HIV-1 pseudoviruses in the presence of inhibitors was measured
448 through HIV-1 pseudoviral tat-induced luciferase production in TZM-bl cells as described
449 previously.⁶⁸ TZM-bl cells were plated at 9000 cells/well into 96 well plates (excluding outer
450 wells to avoid edge effects) followed by overnight incubation at 37°C, 5% CO₂. Inhibitors and
451 pseudoviral particles at a final concentration of 1x (based on TCID₅₀ measurements) were
452 incubated together for 20 min prior to transfer to adherent TZM-bl cells followed by 48 hours
453 incubation at 37°C, 5% CO₂. Viral infection was quantified based on luminescent readings taken
454 immediately after the addition of BrighGlo luciferin substrate to infected cells in lysis buffer and
455 relative infectivity rates calculated based on infectious and noninfectious vehicle control wells
456 (1% DMSO). Antiviral IC₅₀ values were calculated from compound dilution series ran in
457 triplicate.

458 **5.7 HIV Full virus Screening (EASY-HIT).**

459 The EASY-HIT assay³⁵ is based on HIV-1 susceptible reporter cells (LC5-RIC) that contain
460 a stably integrated fluorescent reporter gene that is activated upon successful HIV-1 infection
461 and expression of the early viral protein Rev and Tat. Briefly, LC5-RIC cells were seeded into
462 black 96-well plates at a density of 10,000 cells per well 24 hours prior to infection. Compounds
463 stocks dissolved at 20 mM in DMSO were screened at multiple concentrations from 0.1 to 200
464 μM at a final DMSO concentration of 1% to establish IC₅₀ curves. After compound addition,
465 LC5-RIC cells were infected by adding HIV-1 inoculum at an MOI of 0.5 to each well of the
466 plate. Cells were incubated at 37°C, 5% CO₂ for 48 hours after infection and then measured for

467 reporter expression. Reporter expression was determined by measuring the total fluorescent
468 signal intensity of each well using a fluorescence microplate reader at an excitation filter
469 wavelength of 552 nm and an emission filter wavelength of 596 nm.

470 **5.8 Cell viability assays.**

471 Cell viability of TZM-bl cells was determined by monitoring mitochondrial reductase
472 activity from the reduction of the tetrazolium salt MTT by metabolically active cells.⁶⁹ TZM-bl
473 cells were plated into 96 well plates (Greiner Bio-One) followed by overnight incubation at
474 37°C, 5% CO₂. Compounds were added to wells with a final DMSO concentration of 1%
475 followed by an additional 48 hours incubation. After the designated incubation time, MTT
476 reagent (5mg/mL in 1x PBS) was added to each well to a final concentration of 0.5 mg/mL.
477 MTT containing plates were incubated for an additional 3 hours after which the media was
478 removed, and the reduced purple formazan product dissolved in 50 µL DMSO. Absorbance was
479 measured at 550 nm. Metabolic activity of vehicle-treated cells (1% DMSO) was defined as
480 100% cell growth. Cell viability of LC5-RIC cultures exposed to HIV inoculum and test
481 compounds was determined by performing a CellTiter-Blue® cell viability assay (Promega) and
482 monitoring the ability of metabolically active cells to convert the redox dye resazurin into the
483 fluorescent product resorufin. LC5-RIC cells were plated into black 96 well plates (Greiner Bio-
484 One) followed by overnight incubation at 37°C, 5% CO₂. Compounds stocks dissolved at 20 mM
485 in DMSO were screened at multiple concentrations from 0.1 to 200 µM at a final DMSO
486 concentration of 1% followed by an additional 48 hours incubation. After the designated
487 incubation time, CTB reagent (1:5 in cell culture medium) was added to each well. CTB
488 containing plates were incubated for an additional hour after which fluorescence signal of

489 resazurin was measured using a fluorescence microplate reader at an excitation filter wavelength
490 of 550 nm and an emission filter wavelength of 600 nm.

491 **5.9 Time-of-addition assay.**

492 To gain a further understanding of the mechanism of action of the antiviral azaBINOL
493 compound **B#24**, a time-of-addition experiment was employed utilizing single-round HIV-1
494 pseudo particles.^{70, 71} TZM-bl cells were plated into 96 well plates (Greiner Bio-One) followed
495 by overnight incubation at 37°C and 5% CO₂. After 24 hours, plated TZM-bl cell were infected
496 with HIV-1_{YU2} pseudovirus. **B#24** (60 μM), temsavir (40 nM), efavirenz (40 nM), and raltegravir
497 (1 μM) were added to separate wells at the initial viral inoculation time or at set points post-
498 infection (up to 12 hours post-infection). Cells, virus, and inhibitor were incubated for an
499 additional 48 hours followed by quantification of luciferase production to assess viral infection
500 rates. The antiretroviral drug controls chosen (temsavir, efavirenz, raltegravir) reflect inhibition
501 of HIV-1 at different stages of the viral lifecycle (entry/fusion, reverse transcription, and
502 integration, respectively) allowing for a mechanistic comparison to the unknown antiviral
503 compound **B#24**.

504 **5.10 HIV-1 integrase enzyme assay.**

505 Inhibition of HIV-1 integrase was assessed using an HIV-1 integrase assay kit (XpressBio
506 Life Science Products) according to the manufacturer's instructions. IC₅₀ values were determined
507 through a two-fold dilution series run in triplicate. The normalized percent integrase inhibition
508 was determined using positive and negative control references with a set amount of vehicle
509 solvent (1% DMSO).

510 **5.11 HIV-1 reverse transcriptase enzyme assay.**

511 Antiviral azaBINOL **B#24** was assessed for inhibition of HIV-1 reverse transcriptase using a
512 commercially available colorimetric reverse transcriptase assay kit (Roche) according to the
513 manufacturer's instructions. IC₅₀ values were determined through a dilution series run in
514 triplicate. Normalized percentages of inhibitory activity were calculated using positive and
515 negative control wells with a set amount of vehicle solvent (10% DMSO).

516 **5.12 Polymerase-Independent RNase H assay.**

517 A FRET based assay to assess RNase H inhibition of HIV-1 RT was used as previously
518 described.⁴⁰ In a 100 µL reaction containing 50 mM Tris HCl at pH 7.8, 5.8 M MgCl₂, 1 M
519 dithiothreitol (DTT), 80 mM KCl, 2 nM HIV-1 RT (NIH Aids Reagent, cat#3555), and 0.25 µM
520 annealed RNA/DNA hybrid (5'-GAU CUG AGC CUG GGA GCU-Fluorescein-3'; 5'-Dabcyl-
521 AGC TCC CAG GCT CAG ATC-3'; Metabion, Germany) was incubated at 37°C for 1 hour.
522 Enzymatic activity was quenched with the addition of 50 µL of ethylenediaminetetraacetic acid
523 (EDTA; 0.5 M, pH 8.0) and fluorescence read using a Biotek plate reader at 490/528 nm
524 excitation/emission wavelength. Data was analyzed by subtracting the value of a vehicle blank
525 (1% DMSO) and reporting inhibitor as a percentage of the control.

526 **5.13 Bio-layer interferometry binding analysis.**

527 Binding of compounds to HIV-1 reverse transcriptase was detected and monitored in real
528 time using a FortéBio Octet Red 96 BioLayer Interferometer. Recombinant wildtype HIV-1 RT
529 (NIH Aids Reagent, cat# 3555) was immobilized on amine reactive sensors (AR2G) at 25 µg/mL
530 for 1600 seconds in 50 mM acetate buffer at a pH of 7. Compounds at 20 mM in DMSO were
531 diluted to final concentrations in black 96 well plates (Greiner Bio-One) at a final consistent
532 DMSO concentration of 5% in 1x kinetic buffer (PBS pH 7.4, 0.02% Tween-20, 0.1% albumin,
533 and 0.05% sodium azide, FortéBio). Binding affinity (K_D) was characterized through the analysis

534 of association and dissociation curves at multiple concentrations. All samples were tested in
535 duplicate. Rilpivirine was used as a positive binding control, raltegravir as a negative control.
536 Effects from non-specific binding were removed using double referencing. Residual baseline
537 drift was calculated by fitting the response during baseline periods to an exponential decay and
538 then subtracting this drift. The resulting response curves were globally fit to a 1:1 Langmuir
539 model.⁷² All fits were performed using a constrained, non-linear least squares minimization
540 (MATLAB R2018a, lsqnonlin function implementing the trust region reflective algorithm).
541 Constraints on parameters were used to guide convergence away from non-physical parameter
542 values, but all constraints were inactive at the converged optimum. A parametric bootstrap
543 analysis was used to compute a 95% confidence interval for the computed K_D values, using a
544 normally-distributed error with variance estimated from the sum of squared residuals of the
545 model fit (MATLAB R2018a, 100 iterations). Random noise in response curves was filtered
546 prior to plotting using a smoothing spline (MATLAB R2018a, spaps function).

547 **5.14 Bivalent metal binding assay.**

548 Testing for complexation of **B#24** with Mg^{2+} ions was carried out following previous
549 protocols with adjustments.⁵⁰ In brief, a 1 M stock solution of $MgCl_2$ and a 1 M solution of **B#24**
550 were prepared in 1:1 ethanol/acetonitrile mixtures. **B#24** was diluted to 100 μM and UV
551 absorbance readings recorded using a BioTek synergy plate reader from 200 – 400 nm. 10 μL
552 additions of a 500 mM Mg^{2+} solution containing 100 μM **B#24** (to keep compound concentration
553 consistent) was added stepwise followed by absorbance readings between each addition. The
554 concentration of Mg^{2+} was raised with each addition from 0.5 mM to 120 mM. Alignment,
555 reference subtraction of blanks, and plotting were done on raw data using Microsoft Excel.

556 **5.15 Luminescence inhibition assays.**

557 To determine if **B#24** was capable of non-specifically inhibiting luciferase activity in the
558 HIV-1 pseudotyped assay, we implemented a cell-free assay with purified recombinant luciferase
559 (Promega) and luciferin (BrightGlo Luciferase Assay System; Promega) following a previous
560 protocol.³⁸ Protein and reagents were prepared and stored according to manufacturer's
561 instructions. Preliminary experiments established the concentration of luciferin to be used in the
562 assay in order to closely mimic the protein signal in single-round infectivity assay and give
563 maximal sensitivity in luminescence readings. Reactions were carried out in white 96 well-plates
564 (Gibco; ThermoFisher Scientific) by combining compounds with 0.5 µg/mL recombinant
565 luciferase in 1x PBS buffer and 1 mg/mL BSA (VWR). Reactions were initiated by the addition
566 of 30 µL luciferin substrate to wells. Luminescence readings were immediately recorded and
567 normalized using appropriate controls with vehicle solvent (1% DMSO). The compounds
568 Luciferase Inhibitor I (VWR) and raltegravir (NIH Aids Reagent Program) were used as positive
569 and negative controls respectively.

570 **5.16 Compound aggregation assessment.**

571 We observed precipitation of some azaBINOL compounds at concentrations higher than 200
572 µM in cell media with 1% DMSO. To assess if the antiviral activity from the active azaBINOL
573 compound **B#24** could be due to non-specific aggregation effects, an ¹H-NMR assay was
574 implemented to characterize compound behavior in aqueous conditions as described
575 previously.³⁹ Briefly, **B#24** was solubilized in DMSO-D₆ (MilliporeSigma; Burlington, MA) to a
576 concentration of 20 mM. Serial dilution in 50 mM sodium phosphate at pH 6.8 in 100% D₂O
577 (MilliporeSigma; Burlington, MA) yielded five samples ranging in concentration from 200 µM
578 to 12 µM. ¹H-NMR spectra of each sample was obtained over 64 scans on a Bruker Ascend 800

579 MHz spectrometer equipped with a 5mm TCI cryoprobe. Data was analyzed and plotted using
580 Bruker TopSpin software.

581

582 **Author contributions**

583 All compounds were synthesized and characterized by SB, SMS, and PRB. All cell-based assays
584 were done by RO, GN, and AH. Data analysis was performed by RO, AH, JS, RBW, PRB and
585 SL. The manuscript was written through contributions of all authors and all authors have given
586 approval to the final version of the manuscript.

587

588 **Acknowledgments**

589 This work was supported by OSU start-up funds (SL). Envelope plasmids (pHxB2, pYU2,
590 p89.6) were a kind gift from Carole Bewley (NIH, NIDDK). Temsavir was kindly provided by
591 Bristol Myers Squibb. This compound has subsequently been by acquired by ViiV Healthcare.
592 The following reagents were obtained through the NIH AIDS Reagent Program, Division of
593 AIDS, NIAID, NIH: TZM-bl cells (Cat# 8129) from Dr. John C. Kappes, Dr. Xiaoyun Wu and
594 Tranzyme Inc. Raltegravir (Cat # 11680) from Merck & Company, Inc. Efavirenz (Cat # 4624)
595 from the Division of AIDS, NIAID. Rilpivirine (Cat # 12147) from Tibotec Pharmaceuticals,
596 Inc. HIV-1 RT (Cat #3555) from Dr. Stuart Le Grice and Dr. Jennifer T. Miller. We
597 acknowledge the support of the Oregon State University NMR facility funded in part by the
598 National Institutes of Health, HEI Grant 1S110OD018518, and by the M. J. Murdock Charitable
599 Trust grant #2014162.

600

601 **Supplementary data**

602 Supplementary data (additional NMR data and figures illustrating compound library antiviral
603 screening, protein assay results, BLI control data, and assessment of nonspecific inhibition)
604 associated with this article can be found in the online version.

605

606 **References**

- 607 (1) *HIV/AIDS factsheet*; World Health Organization:
608 <http://www.who.int/mediacentre/factsheets/fs360/en/> 2018.
- 609 (2) Fauci, A. S. An HIV vaccine is essential for ending the HIV/AIDS pandemic. *Jama* **2017**,
610 318, 1535-1536.
- 611 (3) Pham, Q. D.; Wilson, D. P.; Law, M. G.; Kelleher, A. D.; Zhang, L. Global burden of
612 transmitted HIV drug resistance and HIV-exposure categories: a systematic review and meta-
613 analysis. *AIDS* **2014**, 28, 2751-2762.
- 614 (4) Tang, M. W.; Shafer, R. W. HIV-1 antiretroviral resistance. *Drugs* **2012**, 72, e1-e25.
- 615 (5) Miller, C.; Crain, J.; Tran, B.; Patel, N. Rilpivirine: a new addition to the anti-HIV-1
616 armamentarium. *Drugs Today (Barc)* **2011**, 47, 5-15.
- 617 (6) Murphy, R. L.; Montaner, J. Drug Evaluations Anti-infectives: Nevirapine: A review of its
618 development, pharmacological profile and potential for clinical use. *Expert Opin. Investig.*
619 *Drugs*. **1996**, 5, 1183-1199.
- 620 (7) De Clercq, E.; Li, G. Approved antiviral drugs over the past 50 years. *Clin. Microbiol. Rev.*
621 **2016**, 29, 695-747.
- 622 (8) Corona, A.; Masaoka, T.; Tocco, G.; Tramontano, E.; Le Grice, S. F. Active site and
623 allosteric inhibitors of the ribonuclease H activity of HIV reverse transcriptase. *Future Med.*
624 *Chem.* **2013**, 5, 2127-2139.
- 625 (9) Wang, X.; Gao, P.; Menendez-Arias, L.; Liu, X.; Zhan, P. Update on recent developments
626 in small molecular HIV-1 RNase H inhibitors (2013-2016): opportunities and challenges. *Curr.*
627 *Med. Chem* **2018**, 25, 1682-1702.
- 628 (10) de Béthune, M.-P. Non-nucleoside reverse transcriptase inhibitors (NNRTIs), their
629 discovery, development, and use in the treatment of HIV-1 infection: a review of the last 20
630 years (1989–2009). *Antivir. Res.* **2010**, 85, 75-90.
- 631 (11) Beilhartz, G. L.; Götte, M. HIV-1 ribonuclease H: structure, catalytic mechanism and
632 inhibitors. *Viruses* **2010**, 2, 900-926.
- 633 (12) Brunel, J. M. BINOL: a versatile chiral reagent. *Chem. Rev.* **2005**, 105, 857-897.
- 634 (13) Aldemir, H.; Richarz, R.; Gulder, T. A. The biocatalytic repertoire of natural biaryl
635 formation. *Angew. Chem. Int. Ed. Engl.* **2014**, 53, 8286-8293.
- 636 (14) Bringmann, G.; Gulder, T.; Gulder, T. A. M.; Breuning, M. Atroposelective total synthesis
637 of axially chiral biaryl natural products. *Chem. Rev.* **2011**, 111, 563-639.
- 638 (15) Boyd, M. R.; Hallock, Y. F.; Cardellina, J. H.; Manfredi, K. P.; Blunt, J. W.; McMahon, J.
639 B.; Buckheit Jr, R. W.; Bringmann, G.; Schäffer, M.; Cragg, G. M. Anti-HIV michellamines
640 from *Ancistrocladus korupensis*. *J. Med. Chem.* **1994**, 37, 1740-1745.
- 641 (16) Hallock, Y. F.; Manfredi, K. P.; Dai, J.-R.; Cardellina, J. H.; Gulakowski, R. J.; McMahon,
642 J. B.; Schäffer, M.; Stahl, M.; Gulden, K.-P.; Bringmann, G. Michellamines D– F, new HIV-
643 inhibitory dimeric naphthylisoquinoline alkaloids, and korupensamine E, a new antimalarial
644 monomer, from *Ancistrocladus korupensis*. *J. Nat. Prod.* **1997**, 60, 677-683.
- 645 (17) Manfredi, K. P.; Blunt, J. W.; Cardellina, J. H.; McMahon, J. B.; Pannell, L. L.; Cragg, G.
646 M.; Boyd, M. R. Novel alkaloids from the tropical plant *Ancistrocladus abbreviatus* inhibit cell
647 killing by HIV-1 and HIV-2. *J. Med. Chem.* **1991**, 34, 3402-3405.

- 648 (18) Bringmann, G.; Steinert, C.; Feineis, D.; Mudogo, V.; Betzin, J.; Scheller, C. HIV-
649 inhibitory michellamine-type dimeric naphthylisoquinoline alkaloids from the Central African
650 liana *Ancistrocladus congolensis*. *Phytochemistry* **2016**, 128, 71-81.
- 651 (19) McMahan, J. B.; Currens, M. J.; Gulakowski, R. J.; Buckheit, R.; Lackman-Smith, C.;
652 Hallock, Y. F.; Boyd, M. R. Michellamine B, a novel plant alkaloid, inhibits human
653 immunodeficiency virus-induced cell killing by at least two distinct mechanisms. *Antimicrob.*
654 *Agents Chemother.* **1995**, 39, 484-488.
- 655 (20) Bringmann, G.; Holenz, J.; Wiesen, B.; Nugroho, B. W.; Proksch, P. Diconcophylline A as
656 a growth-retarding agent against the herbivorous insect *Spodoptera littoralis*: structure-activity
657 relationships. *J. Nat. Prod.* **1997**, 60, 342-437.
- 658 (21) Teissier, E.; Zandomenighi, G.; Loquet, A.; Lavillette, D.; Lavergne, J. P.; Montserret, R.;
659 Cosset, F. L.; Bockmann, A.; Meier, B. H.; Penin, F.; Pecheur, E. I. Mechanism of inhibition of
660 enveloped virus membrane fusion by the antiviral drug arbidol. *PLoS One* **2011**, 6, e15874.
- 661 (22) Emileh, A.; Tuzer, F.; Yeh, H.; Umashankara, M.; Moreira, D. R.; Lalonde, J. M.; Bewley,
662 C. A.; Abrams, C. F.; Chaiken, I. M. A model of peptide triazole entry inhibitor binding to HIV-
663 1 gp120 and the mechanism of bridging sheet disruption. *Biochemistry* **2013**, 52, 2245-2261.
- 664 (23) Wolf, M. C.; Freiberg, A. N.; Zhang, T.; Akyol-Ataman, Z.; Grock, A.; Hong, P. W.; Li,
665 J.; Watson, N. F.; Fang, A. Q.; Aguilar, H. C.; Porotto, M.; Honko, A. N.; Damoiseaux, R.;
666 Miller, J. P.; Woodson, S. E.; Chantasirivisal, S.; Fontanes, V.; Negrete, O. A.; Krogstad, P.;
667 Dasgupta, A.; Moscona, A.; Hensley, L. E.; Whelan, S. P.; Faull, K. F.; Holbrook, M. R.; Jung,
668 M. E.; Lee, B. A broad-spectrum antiviral targeting entry of enveloped viruses. *Proc. Natl. Acad.*
669 *Sci. U.S.A.* **2010**, 107, 3157-3162.
- 670 (24) Himmel, D. M.; Sarafianos, S. G.; Dharmasena, S.; Hossain, M. M.; McCoy-Simandle, K.;
671 Ilina, T.; Clark Jr, A. D.; Knight, J. L.; Julias, J. G.; Clark, P. K. HIV-1 reverse transcriptase
672 structure with RNase H inhibitor dihydroxy benzoyl naphthyl hydrazone bound at a novel site.
673 *ACS Chem. Biol.* **2006**, 1, 702-712.
- 674 (25) Kankanala, J.; Kirby, K. A.; Liu, F.; Miller, L.; Nagy, E.; Wilson, D. J.; Parniak, M. A.;
675 Sarafianos, S. G.; Wang, Z. Design, synthesis, and biological evaluations of
676 hydroxypyridonecarboxylic acids as inhibitors of HIV reverse transcriptase associated RNase H.
677 *J. Med. Chem.* **2016**, 59, 5051-5062.
- 678 (26) Banerjee, S.; Riggs, B. E.; Zakharov, L. N.; Blakemore, P. R. Synthesis, properties, and
679 enantiomerization behavior of axially chiral phenolic derivatives of 8-(naphth-1-yl)quinoline and
680 comparison to 7,7'-dihydroxy-8,8'-biquinolyl and 1,1'-bi-2-naphthol. *Synthesis* **2015**, 47, 4008-
681 4016.
- 682 (27) Blakemore, P. R.; Kilner, C.; Milicevic, S. D. Harnessing anionic rearrangements on the
683 benzenoid ring of quinoline for the synthesis of 6,6'-disubstituted 7,7'-dihydroxy-8,8'-
684 biquinolyls. *J. Org. Chem.* **2005**, 70, 373-376.
- 685 (28) Blakemore, P. R.; Milicevic, S. D.; Zakharov, L. N. Enzymatic resolution of 7,7'-
686 dihydroxy-8,8'-biquinolyl dipentanoate and its conversion to 2,2'-Di-tert-butyl-7,7'-dihydroxy-
687 8,8'-biquinolyl. *J. Org. Chem.* **2007**, 72, 9368-9371.
- 688 (29) Wang, C.; Flanagan, D. M.; Zakharov, L. N.; Blakemore, P. R. Synthesis of 7,7'-
689 dihydroxy-8,8'-biquinolyl (azaBINOL) via Pd-catalyzed directed double C-H functionalization
690 of 8,8'-biquinolyl: emergence of an atropis from a tropis State. *Org. Lett.* **2011**, 13, 4024-4027.

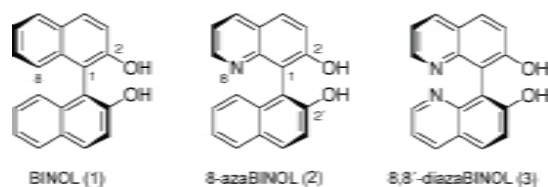
- 691 (30) Blakemore, P. R.; Kilner, C.; Milicevic, S. D. Resolution, enantiomerization kinetics, and
692 chiroptical properties of 7,7'-dihydroxy-8,8'-biquinolyl. *J. Org. Chem.* **2006**, 71, 8212-8218.
- 693 (31) Blakemore, P. R.; Milicevic, S. D.; Perera, H.; Shvarev, A.; Zakharov, L. N. Determination
694 of pKa values for diether derivatives of 7,7'-dihydroxy-8,8'-biquinolyl: dependence of basicity on
695 interannular dihedral angle. *Synthesis* **2008**, 2271-2277.
- 696 (32) Sephton, S. M.; Wang, C.; Zakharov, L. N.; Blakemore, P. R. Silylcyanation of aldehydes,
697 ketones, and imines catalyzed by a 6,6'-bis-sulfonamide derivative of 7,7'-dihydroxy-8,8'-
698 biquinolyl (azaBINOL). *Eur. J. Org. Chem.* **2012**, 2012, 3249-3260.
- 699 (33) Wu, Z.; Wang, C.; Zakharov, L. N.; Blakemore, P. R. Enantioselective synthesis of biaryl
700 compounds via Suzuki-Miyaura cross-coupling using a palladium complex of 7'-butoxy-7-
701 (diphenylphosphino)-8,8'-biquinolyl: investigation of a new chiral ligand architecture. *Synthesis*
702 **2014**, 46, 678-685.
- 703 (34) Harrigan, P. R.; Stone, C.; Griffin, P.; Nájera, I.; Bloor, S.; Kemp, S.; Tisdale, M.; Larder,
704 B. Resistance profile of the human immunodeficiency virus type 1 reverse transcriptase inhibitor
705 abacavir (1592u89) after monotherapy and combination therapy. *J. Infect. Dis.* **2000**, 181, 912-
706 920.
- 707 (35) Kremb, S.; Helfer, M.; Heller, W.; Hoffmann, D.; Wolff, H.; Kleinschmidt, A.; Cepok, S.;
708 Hemmer, B.; Durner, J.; Brack-Werner, R. EASY-HIT: HIV full-replication technology for
709 broad discovery of multiple classes of HIV inhibitors. *Antimicrob. Agents Chemother.* **2010**, 54,
710 5257-5268.
- 711 (36) Baell, J. B. Feeling nature's PAINS: Natural products, natural product drugs, and pan
712 assay interference compounds (PAINS). *J. Nat. Prod.* **2016**, 79, 616-628.
- 713 (37) Auld, D. S.; Southall, N. T.; Jadhav, A.; Johnson, R. L.; Diller, D. J.; Simeonov, A.;
714 Austin, C. P.; Inglese, J. Characterization of chemical libraries for luciferase inhibitory activity.
715 *J. Med. Chem.* **2008**, 51, 2372-2386.
- 716 (38) Bedford, R.; LePage, D.; Hoffmann, R.; Kennedy, S.; Gutschenritter, T.; Bull, L.;
717 Sujjantararat, N.; DiCesare, J. C.; Sheaff, R. J. Luciferase inhibition by a novel naphthoquinone. *J.*
718 *Photochem. Photobiol.* **2012**, 107, 55-64.
- 719 (39) LaPlante, S. R.; Carson, R.; Gillard, J.; Aubry, N.; Coulombe, R.; Bordeleau, S.; Bonneau,
720 P.; Little, M.; O'Meara, J.; Beaulieu, P. L. Compound aggregation in drug discovery:
721 implementing a practical NMR assay for medicinal chemists. *J. Med. Chem.* **2013**, 56, 5142-
722 5150.
- 723 (40) Parniak, M. A.; Min, K.-L.; Budihas, S. R.; Le Grice, S. F.; Beutler, J. A. A fluorescence-
724 based high-throughput screening assay for inhibitors of human immunodeficiency virus-1
725 reverse transcriptase-associated ribonuclease H activity. *Anal. Biochem.* **2003**, 322, 33-39.
- 726 (41) Corona, A.; Tramontano, E. RNase H polymerase-independent cleavage assay for
727 evaluation of RNase H activity of reverse transcriptase enzymes. *Bio Protoc.* **2015**, 5, e1561.
- 728 (42) Klumpp, K.; Hang, J. Q.; Rajendran, S.; Yang, Y.; Derosier, A.; Wong Kai In, P.; Overton,
729 H.; Parkes, K. E.; Cammack, N.; Martin, J. A. Two-metal ion mechanism of RNA cleavage by
730 HIV RNase H and mechanism-based design of selective HIV RNase H inhibitors. *Nucleic Acids*
731 *Res.* **2003**, 31, 6852-6859.
- 732 (43) Budihas, S. R.; Gorshkova, I.; Gaidamakov, S.; Wamiru, A.; Bona, M. K.; Parniak, M. A.;
733 Crouch, R. J.; McMahon, J. B.; Beutler, J. A.; Le Grice, S. F. Selective inhibition of HIV-1

- 734 reverse transcriptase-associated ribonuclease H activity by hydroxylated tropolones. *Nucleic*
735 *Acids Res.* **2005**, 33, 1249-1256.
- 736 (44) Beilhartz, G. L.; Ngure, M.; Johns, B. A.; DeAnda, F.; Gerondelis, P.; Götte, M. Inhibition
737 of the ribonuclease H activity of HIV-1 reverse transcriptase by GSK5750 correlates with slow
738 enzyme-inhibitor dissociation. *J. Biol. Chem.* **2014**, 289, 16270-16277.
- 739 (45) Vernekar, S. K. V.; Tang, J.; Wu, B.; Huber, A. D.; Casey, M. C.; Myshakina, N.; Wilson,
740 D. J.; Kankanala, J.; Kirby, K. A.; Parniak, M. A. Double-winged 3-hydroxypyrimidine-2, 4-
741 diones: potent and selective inhibition against HIV-1 RNase H with significant antiviral activity.
742 *J. Med. Chem.* **2017**, 60, 5045-5056.
- 743 (46) Boyer, P. L.; Smith, S. J.; Zhao, X. Z.; Das, K.; Gruber, K.; Arnold, E.; Burke, T. R.;
744 Hughes, S. H. Developing and evaluating inhibitors against the RNase H active site of HIV-1
745 RT. *J. Virol.* **2018**, 92, 02203-02217.
- 746 (47) Tramontano, E.; Esposito, F.; Badas, R.; Di Santo, R.; Costi, R.; La Colla, P. 6-[1-(4-
747 Fluorophenyl) methyl-1H-pyrrol-2-yl]-2, 4-dioxo-5-hexenoic acid ethyl ester a novel diketo
748 acid derivative which selectively inhibits the HIV-1 viral replication in cell culture and the
749 ribonuclease H activity in vitro. *Antivir. Res.* **2005**, 65, 117-124.
- 750 (48) Chung, S.; Wendeler, M.; Rausch, J. W.; Beilhartz, G.; Gotte, M.; O'Keefe, B. R.;
751 Bermingham, A.; Beutler, J. A.; Liu, S.; Zhuang, X. Structure-activity analysis of vinylogous
752 urea inhibitors of human immunodeficiency virus-encoded ribonuclease H. *Antimicrob. Agents*
753 *Chemother.* **2010**, 54, 3913-3921.
- 754 (49) Masaoka, T.; Chung, S.; Caboni, P.; Rausch, J. W.; Wilson, J. A.; Taskent-Sezgin, H.;
755 Beutler, J. A.; Tocco, G.; Le Grice, S. F. Exploiting drug-resistant enzymes as tools to identify
756 thienopyrimidinone inhibitors of human immunodeficiency virus reverse transcriptase-associated
757 ribonuclease H. *J. Med. Chem.* **2013**, 56, 5436-5445.
- 758 (50) Poongavanam, V.; Corona, A.; Steinmann, C.; Scipione, L.; Grandi, N.; Pandolfi, F.; Di
759 Santo, R.; Costi, R.; Esposito, F.; Tramontano, E. Structure-guided approach identifies a novel
760 class of HIV-1 ribonuclease H inhibitors: binding mode insights through magnesium
761 complexation and site-directed mutagenesis studies. *MedChemComm* **2018**, 9, 562-575.
- 762 (51) Wendeler, M.; Lee, H.-F.; Bermingham, A.; Miller, J. T.; Chertov, O.; Bona, M. K.;
763 Baichoo, N. S.; Ehteshami, M.; Beutler, J.; O'keefe, B. R. Vinylogous ureas as a novel class of
764 inhibitors of reverse transcriptase-associated ribonuclease H activity. *ACS Chem. Biol.* **2008**, 3,
765 635-644.
- 766 (52) Corona, A.; Desantis, J.; Massari, S.; Distinto, S.; Masaoka, T.; Sabatini, S.; Esposito, F.;
767 Manfroni, G.; Maccioni, E.; Cecchetti, V. Studies on cycloheptathiophene-3-carboxamide
768 derivatives as allosteric HIV-1 ribonuclease H inhibitors. *ChemMedChem* **2016**, 11, 1709-1720.
- 769 (53) Massari, S.; Corona, A.; Distinto, S.; Desantis, J.; Caredda, A.; Sabatini, S.; Manfroni, G.;
770 Felicetti, T.; Cecchetti, V.; Pannecouque, C. From cycloheptathiophene-3-carboxamide to
771 oxazinone-based derivatives as allosteric HIV-1 ribonuclease H inhibitors. *J. Enzyme Inhib.*
772 *Med. Chem.* **2019**, 34, 55-74.
- 773 (54) Shah, N. B.; Duncan, T. M. Bio-layer interferometry for measuring kinetics of protein-
774 protein interactions and allosteric ligand effects. *J. Vis. Exp.* **2014**, e51383.
- 775 (55) Kwong, P. D.; Wyatt, R.; Robinson, J.; Sweet, R. W.; Sodroski, J.; Hendrickson, W. A.
776 Structure of an HIV gp120 envelope glycoprotein in complex with the CD4 receptor and a
777 neutralizing human antibody. *Nature* **1998**, 393, 648-659.

- 778 (56) Richman, D. D.; Wrin, T.; Little, S. J.; Petropoulos, C. J. Rapid evolution of the
779 neutralizing antibody response to HIV type 1 infection. *Proc. Natl. Acad. Sci. U.S.A.* **2003**, 100,
780 4144-4149.
- 781 (57) Kwong, P. D.; Mascola, J. R.; Nabel, G. J. Broadly neutralizing antibodies and the search
782 for an HIV-1 vaccine: the end of the beginning. *Nat. Rev. Immunol.* **2013**, 13, 693-701.
- 783 (58) Sluis-Cremer, N.; Arion, D.; Parniak, M. A. Destabilization of the HIV-1 reverse
784 transcriptase dimer upon interaction with N-acyl hydrazone inhibitors. *Mol. Pharmacol.* **2002**,
785 62, 398-405.
- 786 (59) Vernekar, S. K. V.; Liu, Z.; Nagy, E.; Miller, L.; Kirby, K. A.; Wilson, D. J.; Kankanala,
787 J.; Sarafianos, S. G.; Parniak, M. A.; Wang, Z. Design, synthesis, biochemical, and antiviral
788 evaluations of C6 benzyl and C6 biarylmethyl substituted 2-hydroxyisoquinoline-1, 3-diones:
789 dual inhibition against HIV reverse transcriptase-associated RNase H and polymerase with
790 antiviral activities. *J. Med. Chem.* **2014**, 58, 651-664.
- 791 (60) Hang, J. Q.; Li, Y.; Yang, Y.; Cammack, N.; Mirzadegan, T.; Klumpp, K. Substrate-
792 dependent inhibition or stimulation of HIV RNase H activity by non-nucleoside reverse
793 transcriptase inhibitors (NNRTIs). *Biochem. Biophys. Res. Commun.* **2007**, 352, 341-350.
- 794 (61) Bringmann, G.; Gunther, C.; Ochse, M.; Schupp, O.; Tasler, S. Biaryls in nature: a multi-
795 faceted class of stereochemically, biosynthetically, and pharmacologically intriguing secondary
796 metabolites. *Prog. Chem. Org. Nat. Prod.* **2001**, 82, 1-293.
- 797 (62) Platt, E. J.; Bilska, M.; Kozak, S. L.; Kabat, D.; Montefiori, D. C. Evidence that ecotropic
798 murine leukemia virus contamination in TZM-bl cells does not affect the outcome of neutralizing
799 antibody assays with human immunodeficiency virus type 1. *J. Virol.* **2009**, 83, 8289-8292.
- 800 (63) Platt, E. J.; Wehrly, K.; Kuhmann, S. E.; Chesebro, B.; Kabat, D. Effects of CCR5 and
801 CD4 cell surface concentrations on infections by macrophagetropic isolates of human
802 immunodeficiency virus type 1. *J. Virol.* **1998**, 72, 2855-2864.
- 803 (64) Takeuchi, Y.; McClure, M. O.; Pizzato, M. Identification of gammaretroviruses
804 constitutively released from cell lines used for human immunodeficiency virus research. *J. Virol.*
805 **2008**, 82, 12585-12588.
- 806 (65) Wei, X.; Decker, J. M.; Liu, H.; Zhang, Z.; Arani, R. B.; Kilby, J. M.; Saag, M. S.; Wu, X.;
807 Shaw, G. M.; Kappes, J. C. Emergence of resistant human immunodeficiency virus type 1 in
808 patients receiving fusion inhibitor (T-20) monotherapy. *Antimicrob. Agents Chemother.* **2002**,
809 46, 1896-1905.
- 810 (66) Derdeyn, C. A.; Decker, J. M.; Sfakianos, J. N.; Wu, X.; O'Brien, W. A.; Ratner, L.;
811 Kappes, J. C.; Shaw, G. M.; Hunter, E. Sensitivity of human immunodeficiency virus type 1 to
812 the fusion inhibitor T-20 is modulated by coreceptor specificity defined by the V3 loop of gp120.
813 *J. Virol.* **2000**, 74, 8358-8367.
- 814 (67) Le Grice, S. F.; Cameron, C. E.; Benkovic, S. J. Purification and characterization of human
815 immunodeficiency virus type 1 reverse transcriptase. In *Methods in enzymology*, Elsevier: 1995;
816 Vol. 262, pp 130-144.
- 817 (68) Montefiori, D. C. Evaluating neutralizing antibodies against HIV, SIV, and SHIV in
818 luciferase reporter gene assays. *Curr. Protoc. Immunol.* **2005**, 12.11.11-12.11.17.
- 819 (69) Mosmann, T. Rapid colorimetric assay for cellular growth and survival: application to
820 proliferation and cytotoxicity assays. *J. Immunol. Methods* **1983**, 65, 55-63.

- 821 (70) Baldick, C. J.; Wichroski, M. J.; Pendri, A.; Walsh, A. W.; Fang, J.; Mazzucco, C. E.;
822 Pokornowski, K. A.; Rose, R. E.; Eggers, B. J.; Hsu, M.; Zhai, W.; Zhai, G.; Gerritz, S. W.;
823 Poss, M. A.; Meanwell, N. A.; Cockett, M. I.; Tenney, D. J. A novel small molecule inhibitor of
824 hepatitis C virus entry. *PLoS Pathog* **2010**, *6*, e1001086.
- 825 (71) Lara, H. H.; Ayala-Nuñez, N. V.; Ixtapan-Turrent, L.; Rodríguez-Padilla, C. Mode of
826 antiviral action of silver nanoparticles against HIV-1. *J. Nanobiotechnology*. **2010**, *8*, 1-10.
- 827 (72) Oshannessy, D. J.; Brighamburke, M.; Soneson, K. K.; Hensley, P.; Brooks, I.
828 Determination of rate and equilibrium binding constants for macromolecular interactions using
829 surface plasmon resonance: use of nonlinear least squares analysis methods. *Anal. Biochem.*
830 **1993**, *212*, 457-468.
- 831
832

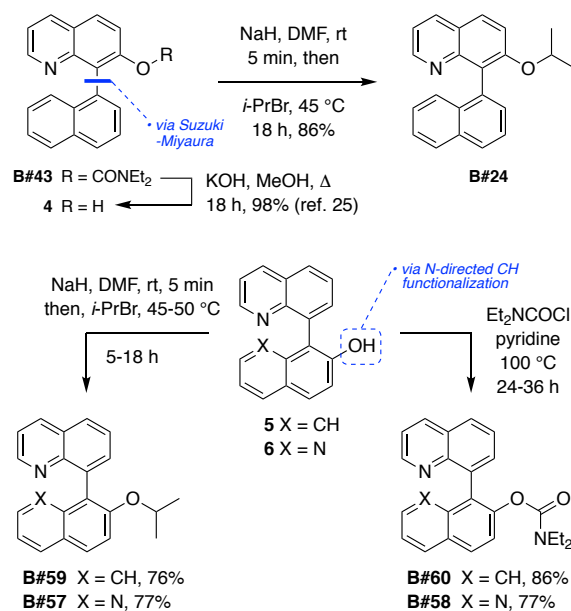
833



834

835

836 **Figure 1.** 1,1'-Bi-2-naphthol (BINOL, **1**) and related 8-(naphth-1-yl)quinoline (**2**) and 8,8'-biquinolyl (**3**) compounds
 837 belonging to the 'azaBINOL' class. The colloquial names '8-azaBINOL' and '8,8'-diazabINOL' conform to BINOL
 838 atom numbering. Molecules are depicted in (*aS*)-configuration and can exist in racemic or scalemic form.
 839



840

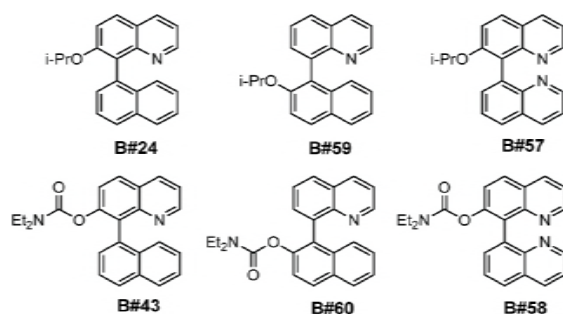
841

842 **Scheme 1.** Synthesis of deoxy-8-azaBINOL (**B#24**, **B#43**, **B#59**, and **B#60**) and 2-deoxy-8,8'-diazabINOL (**B#57**
 843 and **B#58**) derivatives of primary interest for antiviral activity evaluation.

844

845

846



847 **Figure 2.** Structures of selected azaBINOL compounds from synthetic library that show significant antiviral activity
 848 at single dose concentrations (**B#24**, **B#43**, **B#60**) along with closely related congeners showing only modest
 849 antiviral activity (**B#59**, **B#58**, **B#57**).
 850

851
852
853
854
855

Compound	HIV-IC ₅₀ [μM]			CC ₅₀ [μM]	Selectivity Index CC ₅₀ /IC ₅₀
	HxB2	YU2	89.6	TZM-bl	
B#24	6.7 ± 0.9	8.9 ± 0.6	4.7 ± 1.6	68.5 ± 17.1	14.6
B#59	>100	>100	>100	>100	---
B#57	No effect	No effect	No effect	No effect	---
B#43	61.4 ± 3.3	77.6 ± 10.8	56.6 ± 0.8	95.0 ± 13.1	1.7
B#60	12.6 ± 1.6	14.0 ± 0.8	16.8 ± 3.0	69.3 ± 4.9	5.5
B#58	No effect	No effect	No effect	No effect	---

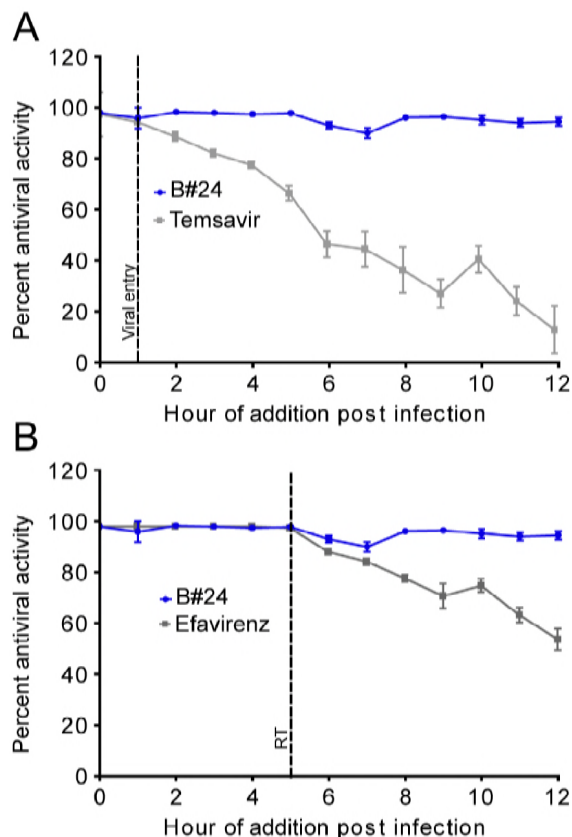
856
857
858
859
860
861

Table 1. HIV-1 pseudo-viral assay determined IC₅₀ and CC₅₀ for selected azaBINOLs.

Compound	IC ₅₀ [μM]	CC ₅₀ [μM]	Selectivity Index CC ₅₀ /IC ₅₀
	HIV-1 _{III} B	LC5-RIC	
B#24	7.6 ± 0.2	86.5 ± 3.7	11.4
B#59	39.5 ± 1.7	144 ± 7.7	3.6
B#57	No effect	No effect	---
B#43	24.1 ± 0.7	51.9 ± 1.2	2.2
B#60	50.1 ± 3.7	71.4 ± 2.8	1.4
B#58	No effect	382.8 ± 166.2	---

862
863
864
865

Table 2. EASY-HIT HIV-1 assay determined IC₅₀ and CC₅₀ for selected azaBINOLs.

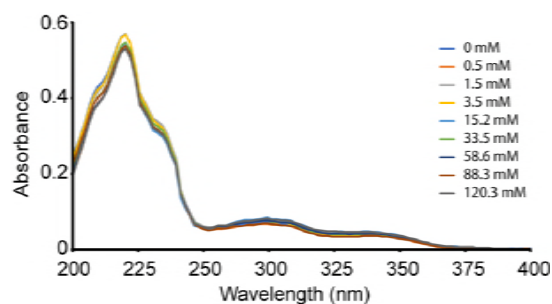


866
867 **Figure 3.** Time-of-addition analysis comparing HIV-1 antiviral activity of **B#24** to antiviral controls at various time
868 points post-infection. TZM-bl cells were infected with HIV-1_{YU2} followed by inoculation with antiviral agents at the
869 indicated time points. A) **B#24** activity profile was compared to an attachment inhibitor (temsavir, 40 nM) and B) a
870 NNRTI (efavirenz, 40 nM). Results are presented as the mean \pm S.D. (*error bars*) of triplicates ($n = 3$).
871
872
873
874

	HIV-1 Integrase	HIV-1 RT	HIV-1 RNase H	<i>E. coli</i> RNase H	MuLV RNase H	AMV RNase H
B#24	>100 μ M	>100 μ M	14.2 \pm 2.8 μ M	44.3 \pm 6.4 μ M	>100 μ M	>100 μ M
B#57	>100 μ M	>100 μ M	>100 μ M	>100 μ M	>100 μ M	>100 μ M
Rilpivirine	-	~1 nM	>10 μ M	>10 μ M	>10 μ M	>10 μ M
Raltegravir	1.1 \pm 0.2 μ M	-	-	-	-	-

875
876
877 **Table 3.** **B#24** shows specific inhibition against RNase H with an IC₅₀ of 14.2 \pm 2.8 μ M. **B#57** does not show
878 inhibition against any enzyme tested. Data shown represent mean \pm S.D. (*error bars*) of triplicates ($n = 3$).
879

880



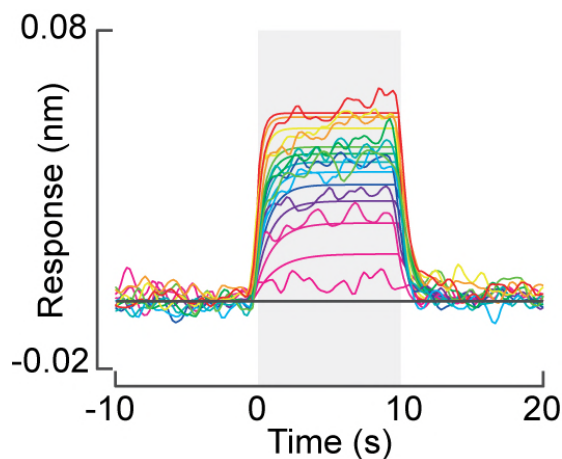
881

882 **Figure 4.** Mg²⁺ ion chelation assay. UV absorbance spectra of **B#24** (100 μM) in the presence of varying
883 concentrations of Mg²⁺ ion. No concentration dependent change of absorbance of **B#24** was seen at any wavelength
884 scanned.

885

886

887



888

889 **Figure 5.** BLI response of inhibitor **B#24** binding to HIV-1 RT enzyme. **B#24** shows a dose-dependent binding
890 to HIV-1 RT with a K_D of 38 μM with a 95% confidence interval between 36 – 41 μM. **B#24** was analyzed at 11
891 concentrations: 10, 20, 30, 40, 50, 60, 70, 80, 120, 160, and 200 μM. Data was fit globally using a 1:1 binding
892 model.